Available online at www.sciencedirect.com

ScienceDirect

Procedia Engineering 170 (2017) 473 – 481

Procedia Engineering

www.elsevier.com/locate/procedia

Engineering Physics International Conference, EPIC 2016

Dynamic Model of Chloralkali Membrane Process

T Budiarto[a], E Esche[a], J U Repke[a], E Leksono[b]

[a] *Process Dynamics and Operations Group, DBTA , Technische Universität Berlin, Str. des 17. Juni 135, D-10623 Berlin, Germany*[*]
[b] *Engineering Physics Group, Institut Teknologi Bandung, Str. Ganesha 10, 40132 Bandung, Indonesia*[†]

Abstract

Chloralkali is one of the most important and energy intensive processes in the chemical industry. The process produces chlorine through electrochemical conversion. The process's energy consumption is a major production cost for the chloralkali industry. Since the demand for energy efficiency and environmentally friendly processes in industry increases, ion exchange membranes are used intensively in the process. One of the prospective energy sources for this process is renewable energy, which shows strong fluctuations and highly unpredictable behavior. Dynamic behavior of the process becomes important to measure and predict the feasibility of the process. Therefore, modelling of the process dynamics is required. Rigorous model of material balance and voltage balance of the process are developed and investigated in this paper. The material transport phenomena inside the electrolyser are modelled considering a number of driving forces. The developed model also predicts the voltage and current density of the cell. The process simulation result is compared to experimental data.

Peer-review under responsibility of the organizing committee of the Engineering Physics International Conference 2016
Keywords: chloralkali; dynamic model; electrochemical process; demand response potential

1. Introduction

By now, renewable energy has become an important component of Germany's energy mix. In 2014, renewable sources amounted to 26.2% of power generation, and this is increasing further due to the German Government requiring the renewable energy share in power generation to reach 40 - 45% by 2025 and 55 - 60% by 2035 [14]. The anourmous share of renewable energy introduces its dynamic characteristics into the whole power grid. An integration with energy storage systems is one of the possible solutions for fluctuating power generation. Unfortunately, the power generation has reached the limit of energy storage's capacity and the produced electricity needs to be consumed in order to save the integrity of the power grid. This condition causes electricity prices to fall below zero. Another possible solution for the overproduction of electricity is a demand response scheme. The chemical industry emerges as one of the potential energy consumers for the latter. Chlorine is one of the most indispensable intermediates in the chemical industry. It is commonly produced through the chloralkali process, which is an electrochemical process that decomposes an aqueous solution of sodium chloride by direct current, producing chlorine gas, hydrogen gas, and sodium hydroxide solution. The process' energy consumption dominates the production costs. Given the large-scale introduction of renewable energy sources in Germany's electrical grid, both energy suppliers as well as consumers must adjust to an increasingly flexible market. Therefore, dynamic operation of the process has become a new issue in recent discussions.

In a previous paper [17], the dynamic characteristic of a chloralkali process has been modelled. The model assumed that the driving force for ion diffusion through the membrane is just the concentration gradient. Toshikatsu Sata [18] explained the significance of the electric potential gradient as an additional driving force of the ionic transport through the ion exchange membrane. In this paper, the process model includes the electric potential as a major driving force for ion transport through the

[*] Thomas Budiarto. *E-mail address:* t.budiarto@campus.tu-berlin.de; Erik Esche. *E-mail address:* erik.esche@tu-berlin.de; Jens-Uwe Repke. *E-mail address:* j.repke@tu-berlin.de
[†] Edi Leksono. *E-mail address:* edi@tf.itb.ac.id

Peer-review under responsibility of the organizing committee of the Engineering Physics International Conference 2016
doi:10.1016/j.proeng.2017.03.076

membrane. The model is compared with experimental data from reference [4]. The dynamic behavior of the chloralkali process is simulated in order to understand the dynamic response of the chloralkali process to an increase of the current density.

2. The Process Model

The chloralkali process consists of two half-cells, which are known as anode cell and cathode cell. In the anode cell, oxidation of chloride ions takes place. And electrons are driven towards the cathode by an external electric potential. Within the cathode cell, the transferred electrons reduce hydronium ions. The chemical reactions, which are considered in the developed model, can be expressed as:

Anode cell: $2Na^+ + 2Cl^- \rightarrow Cl_2 + 2Na^+ + 2e^-$
$2Cl^- \rightarrow Cl_2 + 2e^-$

Cathode cell: $2H_2O + 2e^- \rightarrow H_{2(g)} + OH^-$
$Na^+ + OH^- \rightarrow NaOH_{(aq)}$

Total reaction: $2H_2O + 2NaCl \rightarrow H_{2(g)} + Cl_{2(g)} + 2NaOH_{(aq)}$

The developed model consists of material balances for all ions, liquids and gases and the energy balance in terms of voltage in the electrochemical cell. Figure 1 illustrates the process, which is modelled in this study.

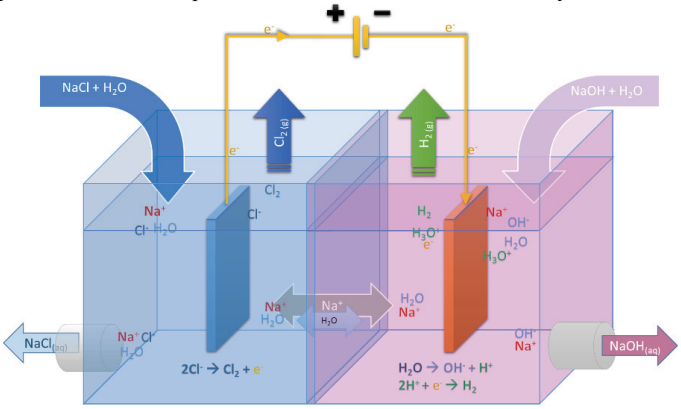

Fig. 1 Diagram of chlor-alkali model

The reactor was modelled as a continuously stirred tank reactor, which makes the electrolyte concentration uniform in each cell compartment. The material balance considers sodium ions, hydroxide ions, water, and chloride. The liquid volume of each half cell is assumed to be constant. Based on Faraday's Law, redox reaction rates in the chlor-alkali cell are estimated with the following expressions:

$$\dot{N}^{H_2}_{CatOut} = \frac{i \cdot A}{2F} \quad (1)$$

$$\dot{N}^{Cl_2}_{AnOut} = \frac{i \cdot A}{2F} \quad (2)$$

wherein $\dot{N}$ is the molar rate of production in kmol/s, and subscript *CatOut* and *AnOut* denote cathode outlet and anode outlet respectively. The model assumes that the current efficiency is 100%, so that the quantity of produced gas flows out of both compartments is equal to the production rate of the gases. The other parallel reactions, which appear to be current inefficiencies, are neglected in this model. Tilak and Chen [2] mention that chlorine gas in the anode might dissolve in water to form soluble chlorine, which hydrolyses to form HOCl and OCl^-. Both of them react further to form ClO_3^-. However, based on reference [3], the solubility of Chlorine in water and a solution of NaCl is below 1% of the solution weight when the solution temperature is above 20 ^oC. In accordance with [3], Fig. 2 shows that the solubility of chlorine in water, HCl solution, and NaCl solution decreases with rising temperature and concentration. Hence, the influence of these parallel reactions is minor compared to the other chloralkali reactions, and can be neglected.

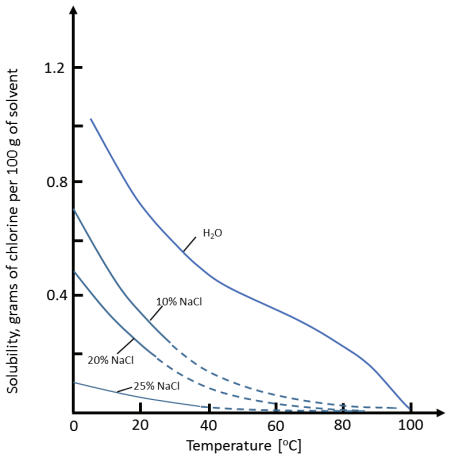

Fig 2. Solubility of chlorine in water, hydrochloric acid, and sodium chloride solutions, in accordance with reference [3].

2.1. Material balance

The developed model assumes that the process and ions transport between the anolyte and catholyte change the volume of neither the catholyte nor anolyte, so that the accumulative volume of the catholyte and anolyte will be assumed to be constant, by making the feed flow rate equal to the outlet flow rate.

2.1.1. Sodium ion balance

Sodium ions in the modelled process mainly originate from feeding electrolytes, which are NaCl and NaOH. The catholyte feed is a lean solution of NaOH and the catholyte outlet has a higher concentration of NaOH. On the other side, the anode feed has a high concentration of NaCl, and the anode outlet has a lean concentration of NaCl. Some of the sodium ions (Na^+) in the anolyte are driven through the membrane [18]. The following equations (Eq. 3, 4, and 5) formulate the sodium ion balance in the cell.

$$\frac{dN^{Na}_{CatAcc}}{dt} = C^{NaOH}_{CatIn}\cdot\dot{V}_{CatIn} - C^{Na}_{CatAcc}\cdot\dot{V}_{CatOut} + A_{mem}\cdot D^{Na}\cdot\left(\frac{C^{Na}_{AnAcc}\cdot F\cdot V_{Cell}}{R\cdot T\cdot\delta} + \frac{C^{Na}_{AnAcc} - C^{Na}_{CatAcc}}{\delta} + C^{Na}_{AnAcc}\frac{\ln\left(\gamma^{NaCl}_{AnAcc}\right) - \ln\left(\gamma^{NaOH}_{CatAcc}\right)}{\delta}\right) \quad (3)$$

$$\frac{dN^{Na}_{AnAcc}}{dt} = C^{NaCl}_{AnIn}\cdot\dot{V}_{AnIn} - C^{Na}_{AnAcc}\cdot\dot{V}_{AnOut} - A_{mem}\cdot D^{Na}\cdot\left(\frac{C^{Na}_{AnAcc}\cdot F\cdot V_{Cell}}{R\cdot T\cdot\delta} + \frac{C^{Na}_{AnAcc} - C^{Na}_{CatAcc}}{\delta} + C^{Na}_{AnAcc}\frac{\ln\left(\gamma^{NaCl}_{AnAcc}\right) - \ln\left(\gamma^{NaOH}_{CatAcc}\right)}{\delta}\right) \quad (4)$$

The driving forces consist of gradients in the electrochemical potentials, which are the chemical potential and the electric potential. The electric potential consists of a voltage difference between both electrodes, which produces an electric field that drives cations into the cathode's direction and anions into the anode's direction. Sata [18] explained the cation flux through the ion exchange membrane and presented the phenomenon in partial differential equations. The third term on the right hand of Eq. 3 and 4 are simplification of those equations. The simplification is acceptable since the electrochemical potentials gradients across the membrane are assumed to be linear.

2.1.2. Hydroxide ion balance

The hydroxide ions are produced by the reduction reaction at the cathode, which breaks water into OH^- and H_3O^+ ions. Based on Faraday's Law, the OH^- production rate is proportional to the electrolysis current that represents the reaction rate. Since the membrane is a cation exchange membrane, only cations can migrate through the membrane. In the practical case [19], the membrane has an ion selectivity factor of at least 98%. The developed model, here, assumes that the selectivity factor is 100%. The OH^- ions then cease to exist in the anode compartment. The hydroxide ion balance in the developed model is written as:

$$\frac{dN^{OH}_{CatAcc}}{dt} = C^{NaOH}_{CatIn}\cdot\dot{V}_{CatIn} + \frac{i\cdot A_{el}}{2F} - \frac{N^{OH}_{CatAcc}}{V_{CatAcc}}\cdot\dot{V}_{CatOut} \quad (5)$$

2.1.3. Chloride balance

The chloride ions enter the anode compartment along with the NaCl solution feed. The ions are consumed in the anolyte by the oxidation reaction on the anode that produces chlorine gas. The reaction rate is estimated by counting the rate of electrons taken by the chloride ion. The accumulated chloride ions in the anolyte is described by the following expression:

[redacted] (6)

2.2. Cell voltage

The chlor-alkali process consumes electrical energy from an external power supply. The process energy consumption is defined by overall cell voltage and the electrolysis current. The value of overall cell voltage is influenced by process variables and cell design, such as activities of the reactants, current density, temperature and distance between both electrodes and membrane. In the developed model, the required cell voltage is the accumulation of the standard electrode potential, activation overpotential, ohmic overpotential. This cell voltage model is described in the following equations:

$$V_{cell} = E + \mu_{act} + \mu_{ohm} \tag{7}$$

$$E = 2.187 - 4.272 \cdot 10^{-4}(T - 25) + \frac{R \cdot T}{2 \cdot F \cdot \alpha} \ln\left(\frac{\left(\gamma_{CatAcc}^{NaOH}\right) \cdot \sqrt{p_{an}^{Cl_2}}}{\sqrt{p_{an}^{H_2}} \cdot \left(\gamma_{AnAcc}^{NaCl}\right)} \right) \tag{8}$$

$$\mu_{act} = \frac{R \cdot T}{2 \cdot F \cdot (1-\alpha)} \ln\left(\frac{i}{i_{an}^{o}}\right) + \frac{R \cdot T}{2 \cdot F \cdot (\alpha)} \ln\left(\frac{i}{i_{cat}^{o}}\right) \tag{9}$$

$$\mu_{ohm} = i \cdot A \cdot R_{cell} \tag{10}$$

$$R_{cell} = \frac{\Delta X}{C_{AnAcc}^{Na} \cdot A_{mem} \cdot (K_{NaCl}^{o} - K_{NaCl}\sqrt{C_{AnAcc}^{NaCl}})} + \frac{\Delta X}{C_{CatAcc}^{Na} \cdot A_{mem} \cdot (K_{NaOH}^{o} - K_{NaOH}\sqrt{C_{CatAcc}^{NaOH}})} + \frac{1}{A_{mem} \cdot K_{mem}} \tag{11}$$

The standard electrode potential was obtained from Nernst' equation, that was adapted for the chlor-alkali case [20]. The standard potential is the minimum potential to overcome the equilibrium potential of the redox reactions in the chloralkali process. The activity coefficients in Eq. (8) were estimated by using a set of equations that was provided by Chandran et. al. [20].

The activation overpotential is a cell voltage that drives the ions in the cell. An increase in the cell's current density results in a higher activation overpotential. This relation was formulated in Eq. 9. The exchange current density of anode (i^{o}_{an}) and cathode (i^{o}_{cat}) in Eq. (9) were estimated by using [22]:

$$\log(i_{cat}^{o}) = (-0.0045 \cdot m_{NaOH}^{2}) + (0.203 \cdot m_{NaOH}) - 5.92 \tag{12}$$

The last part of overall cell voltage is the ohmic overpotential, which is related to the cell's electric resistance and the current density. Both activation and ohmic overpotential represent irreversible parts of the total energy consumption of the process, which convert consumed electricity into heat.

3. Model Validation

The modelling and simulation process is shown by Fig.3. The equations are developed and integrated in the MOSAIC modelling environment. Then, the developed model is simulated in MATLAB.

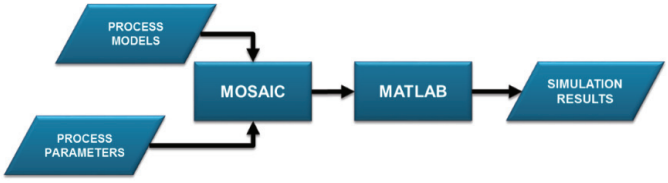

Fig 3. Modelling and Simulation Process Diagram

A model validation was done by comparing steady-state simulation data with experimental data provided by [4]. The model is constructed in MOSAIC and then simulated in MATLAB. Dias [4] measured some variables from a laboratory-scale chloralkali electrolyser to investigate and characterize the membrane cell. The comparison results are expressed in Fig. 4. It shows the polarization curve of the chloralkali cell model and the chloralkali electrolyzer. These figures show that the trend in polarization diagrams of both have similar trends, although there is an offset between the model values and the experimental values.

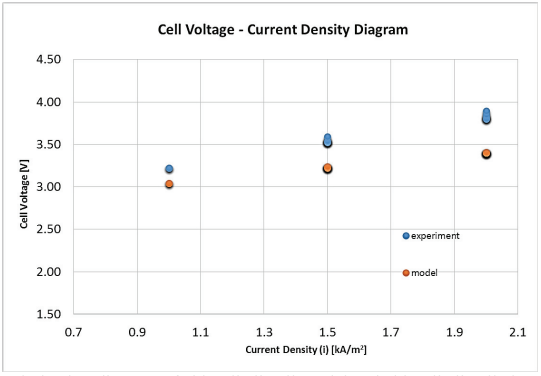

Fig 4. Polarization diagram of chloralkali cell model and chloralkali cell electrolyzer

The offset emerges since the cell voltage model does not consider the hydrodynamics inside the cell compartment. Some references [4], [6], [7], and [8] reported that the existence of bubbles inside the cell compartment influences the cell voltage. Fig. 5(a) shows the influence of the gas void fraction in electrolyte on the cell voltage. Increases in the gas void fraction cause an increase of the cell voltage – this phenomenon also increases the difference between the cell voltage and its theoretical value.

Some references [4], [6], [9], [10], [11], and [12] reported that increasing the volume rate through the cell compartment strengthens the electrolyte circulation and as a result, decreases the gas void effect due to improved gas removal. As expected, the offset between the model and experimental data is lower in the higher circulation rate, as shown in Fig. 5(b).

(a)

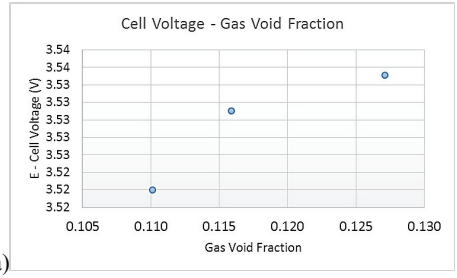

(b)

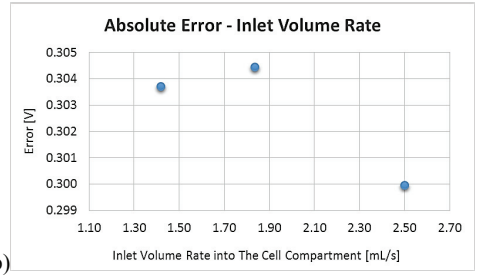

Fig 5. (a) Cell voltage compared to gas void fraction; (b) Absolute error (model bias) compared to gas void fraction

4. Simulation Results and Discussion

Simulations are conducted to investigate the dynamic response of the cell when the current density increases. In the simulation, the cell model, which was validated, is scaled up to a commercial cell scale. The cell design and operation plan are listed in Tab. 1. During the operation, the current density is increased from 1000 A/m^2 to 5000 A/m^2, as shown by Fig. 6(b). The electrolyte volume during the simulation is kept constant. Inlet and outlet volume rates are also constant and balanced. The process was started with concentration of NaCl and NaOH in 5 kmol/m^3.

Table 1. Simulation parameters

Process Parameter	Value
[NaCl] at anode inlet (kmol/m^3)	5.13
[NaOH] at cathode inlet (kmol/m^3)	8.89
A_{el} / Electrode dimension (m^2)	3.4
A_{mem} / Membrane effective area (m^2)	3.4
$\dot{V}_{AnIn}$, $\dot{V}_{AnOut}$, $\dot{V}_{CatIn}$, $\dot{V}_{CatOut}$ (m^3/s)	1 x 10^{-3}
V_{Cat}, V_{An} / volume of electrolyte (m^3)	2.04 x 10^{-2}
α	0.5
D^{Na} (m^2/s)	1.58 x 10^{-10}
D^{H2O} (m^2/s)	1.5 x 10^{-10}
$E^0_{An} - E^0_{Cat}$ (V)	2.187
i (A/m^2)	1000 - 5000
K_{mem} (Siemens)	1.11 x 10^4
R (m^3.kPa/ K.kmol)	8.314
T (K)	348.0
i^0_{an} (A/m^2)	12.5

The simulation results are shown by figures 6, 7 and 8. Fig. 6(a) shows that the standard cell potential contributes the most to the energy cost of the chloralkali process. This part of the energy consumption is used for overcoming the redox reaction potential of the chlor-alkali process.

In the low current density operation regime, activation overpotential is the second biggest energy term after the ohmic overpotential. The activation overpotential is part of the energy consumption that drives the redox reactions in the process. The quantity of the energy cost is a property of the electrode material and the activity of the reactants and products in the process.

As the current density increases, the ohmic overpotential rises and in the specific value of current density, its quantity surpasses the activation potential. This is shown in Fig. 6(a), the ohmic overpotential increases along with current density. Higher current density, which is demanded for increasing plant production rates, results in a lower efficiency and electrical energy converted into heat. From the thermodynamic point of view, this part of the energy consumption increases the entropy generation. Both ohmic overpotential and activation overpotential represent the irreversible energy part of the total energy cost.

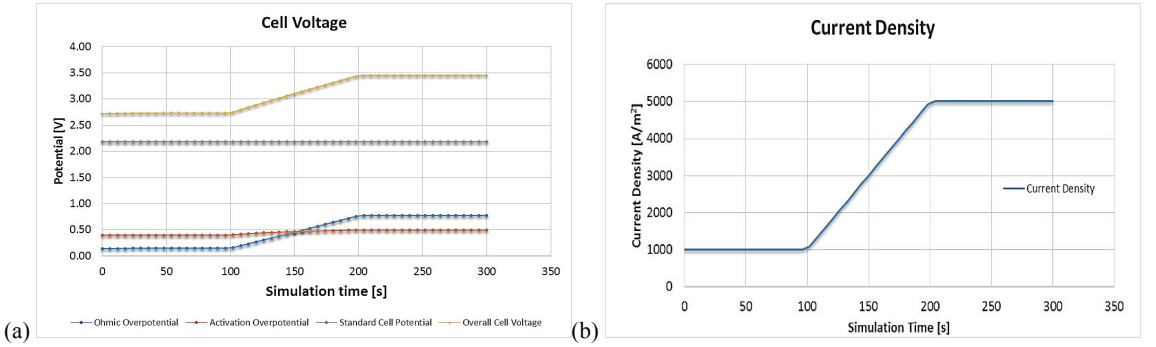

Fig 6. (a) Cell voltage and its distribution; (b) Current density of simulated chloralkali membrane cell.

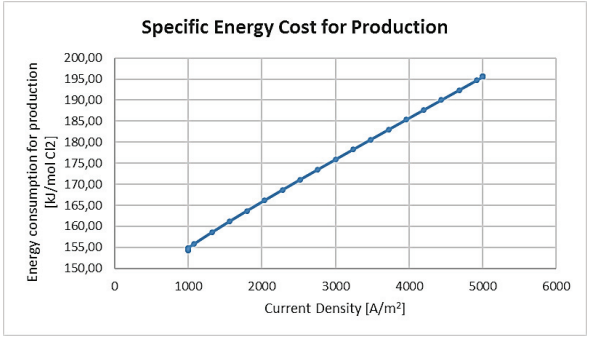

Fig 7. Decomposition potential, activation potential, and ohmic potential of a chloralkali membrane cell, at $\dot{V} = \mathbf{1}\ \boldsymbol{l/s}$

The simulation also shows that the dynamic of production capacity or current density insignificantly influenced the concentration of the process reactants. Although concentration of the Chloride (Cl^-) in the anolyte is influenced by the adjustment of the current density, the trend of reactants concentration majorly follows the concentration of the process inlets and their rate, which are strongly controllable. This phenomenon can be seen in Fig. 8(a), (b), and (c).

As a summary, as shown by Fig. 7, the specific energy cost of chlorine production is increased along with the increase of the current density. The increase is mostly caused by the larger part of the irreversible energy consumption of the process. Though the developed model does not consider the escalation of temperature due to heat generation in the process, the trend is clear, that lower current density operation provides better efficiency in the thermodynamic point of view.

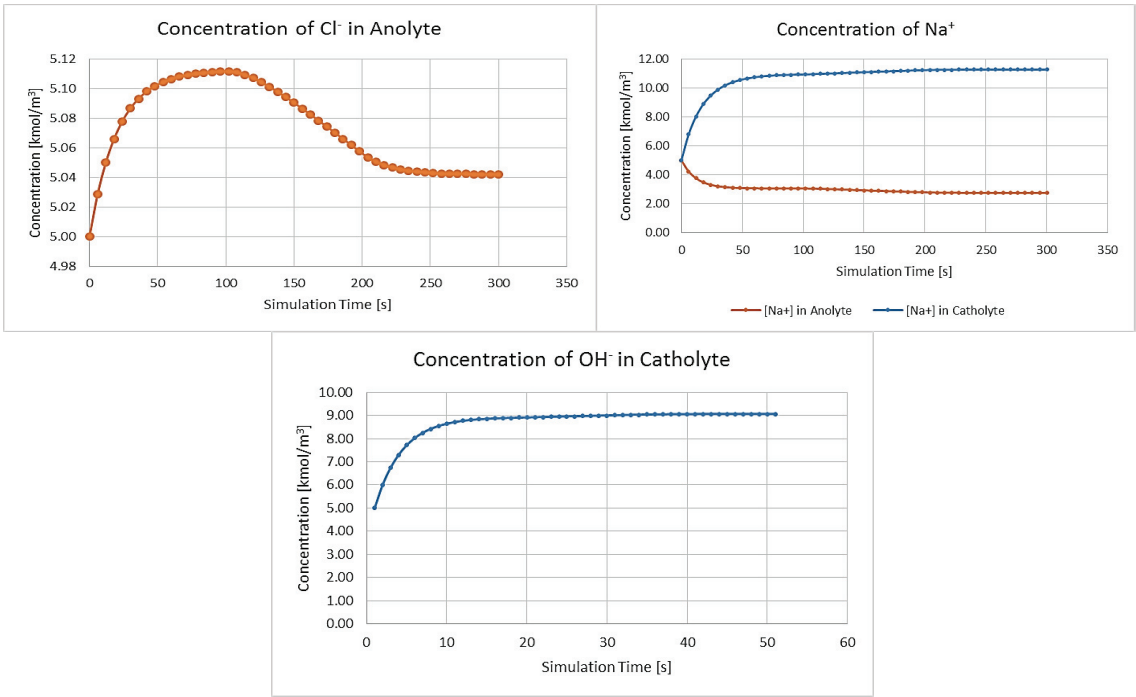

Fig 8. Concentration of process reactants [kmol/m^3]: (1) Concentration of Cl^- in anolyte, (2) Concentration of Na^+ in both anolyte and catholyte, (3) concentration of OH^- in catholyte

5. Conclusion

In order to investigate the demand response potential of the chloralkali membrane process, a dynamic process model of the chloralkali membrane process has been developed in the MOSAIC and MATLAB modeling environment.

The increment of energy input in term of current density is simulated, and energy cost of the process is analyzed. The results show that operation in higher current density increases irreversible part of the energy cost, which increases the specific energy cost for production of Chlorine. Activity of the reactants, which is represented by concentration of the reactants, is insignificantly influenced by the increase of the current density.

For future work, modeling the process in the thermodynamic point of view can be useful to extend the process modeling and integrating the model with other system. Furthermore, it is also important to include the economic consideration in the process performance analysis to quantify the demand response potential in the process.

6. Nomenclature

$\dot{N}^{H2}_{CatOut}$ – production rate of H_2 in the cathode cell (kmol/s)

$\dot{N}^{Cl2}_{AnOut}$ – production rate of Cl_2 in the anode cell (kmol/s)

I – electrolysis current (kA)

F – faraday constant : 96’485 (kCoulomb / kmol e^-)

V_{CatAcc} – accumulative volume of catholyte (m^3)

$\dot{V}_{CatIn}$ – volume rate of cathode inlet (m^3/s)

$\dot{V}_{CatOut}$ – volume rate of cathode outlet (m^3/s)

$\dot{V}_{AnIn}$ – volume rate of anode inlet (m^3/s)

$\dot{V}_{AnOut}$ – volume rate of anode outlet (m^3/s)

N^{Na}_{CatAcc}, N^{Na}_{AnAcc} – mole quantity of Na^+ ion in catholyte and anolyte (kmol)

C^{NaOH}_{CatIn} – concentration of NaOH in the catholyte feed (kmol/m^3)

C^{NaCl}_{AnIn} – concentration of NaCl in the anolyte feed (kmol/m^3)

C^{Na}_{AnAcc} – concentration of Na^+ ion in the anolyte (kmol/m^3)

C^{Na}_{CatAcc} – concentration of Na^+ ion in the catholyte (kmol/m^3)

$\dot{V}_{CatIn}$, $\dot{V}_{AnIn}$ – feeding rate in the cathode and anode compartment (m^3/s)

$\dot{V}_{CatOut}$, $\dot{V}_{AnOut}$ – outlet rate of the cathode and anode compartment (m^3/s)

A – ion diffusion area in the membrane (10^{-2} m^2),

D^{Na} – diffusion coefficient of Na^+ ion in the membrane (4 x $10^{-9}$$m^2$/s)[1]

δ – membrane thickness (2.5 x 10^{-4} m)[4]

N^{OH}_{CatAcc} – mole quantity of OH^- ion (kmol)

C^{NaOH}_{CatIn} – concentration of NaOH in the catholyte feeding (kmol/m^3)

N^{Cl}_{AnAcc} – accumulated Cl- ion in the anode (kmol)

C^{NaCl}_{AnIn} – concentration of NaCl in the anode feeding (kmol/m3)

V_{cell} – cell voltage (Volt)

E – standard electrode potential (Volt)

μ_{act} – activation overpotential (Volt)

μ_{ohm} – Ohmic overpotential (Volt)

$E^0_{An} - E^0_{Cat}$ – standar electrode potential for anode and cathode (Volt)

α – charge transfer coefficient (symmetry factor = 0.5)

T – temperature (K)

R – ideal gas constant : 0.008314 (m^3.Pa/(K.kmol))

i – current density (kA/m^2)

i^0_{an} – exchange current density of anode (kA/m^2)

i^0_{cat} – exchange current density of cathode (kA/m^2)

Acknowledgements

This research is partly supported by *LPDP, Indonesian Endowment Fund for Education*, which is funding the doctoral study of the researcher. And this material is also based upon work supported by *the Process Dynamics and Operations Group at Technische Universität Berlin*, which also provides infrastructure and assistance for researching this topic.

References

[1] Barry A. Friedfeld (author), T. C. Wellington (editor), *Modern Chlor-Alkali Technology*, *Volume 5*, Springer Netherlands, 1992.
[2] B.V. TILAK and C.-P. Chen, *Calculation of the current efciency of the electrolytic sodium chlorate cells*, Journal of Applied Electrochemistry 29 : 1237-1240, Kluwer Academic Publisher, Netherlands, 1999.
[3] Schmittinger P., Florkiewicz T., Curlin L.C., Luke B., et.al., *Ullmann's Encyclopedia of Industrial Chemistry – Chlorine*, Wiley-VCH Verlag GmbH & Co. KGaA, Weinheim, 2012.
[4] Dias, A.C.d.B.V., *Chlor-Alkali Membrane Cell Process*, PhD Disertation, Chemical and Biological Engineering – University of Porto, 2013.
[5] K.L.Hardee, "*A Simple procedure for evaluating membrane electrolyzer performance*", *Modern Chlor-Alkali Technology*, 6, 235-242, 1995.
[6] F. Hine, M. Yasuda, R. Nakamura, T. Noda, *Journal of The Electrochemical Society 122,* 1185-1190, 1975.
[7] Y. Xiong, L. Jialing, S.Hong, *Journal of Applied Electrochemistry 22*, 486-490, 1992.
[8] Ph. Mandin, A. Aissa, H.Roustan, J. Hamburger, G. Picard, *Chemical Engineering and Processing 47*, 1926-1932, 2008.
[9] T. Mirzazadeh, F. Mohammadi, M. Soltanieh, E. Joudaki, *Chemical Engineering Journal, 140,* 157-164, 2008.
[10] N. S. Kaveh, S.N. Ashrafizadeh, F. Mohammadi, *Chemical Engineering Research and Design 86*, 461-472, 2008.
[11] A.A. Jalali, F. Mohammadi, S.N. Ashrafizadeh, *Desalination, 237*, 126-139, 2009.
[12] N. S. Kaveh, F. Mohammadi,, S.N. Ashrafizadeh, *Chemical Engineering Journal 147*, 161–172, 2009.
[13] Marangio F., Santarelli M., Calı` M., *Theoretical model and experimental analysis of a high pressure PEM water electrolyser for hydrogen production*, International Journal of Hydrogen Energy 34, Elesevier, 2009, 1143-1158.
[14] Auer, J., Anatolitis, V., *The Changing energy mix in Germany*. Deutche Bank Research, Curent Issues – Natural Resources, June 26, 2014
[15] Bird R.B., Stewart W.E., Lightfoot E.N., *Transport phenomena 2nd ed*. John Wiley & Sons Inc., 2002.
[16] Springer T.E., Zawodzinski T.A., Gottsfeld S., *Polymer electrolyte fuel cell model*. Journal of Electrochemical Society, 138:2334–41, 1991.
[17] Budiarto, T., Esche, E., Repke, J., *Dynamic Modeling and Operation of The Chlor-Alkali Process*. Czasopismo Techniczne / Technical Transaction, ISSN : 0011-4561. 2016.
[18] Sata, T. *Ion Exchange Membranes : Preparation, Characterization, Modification and Application*. The Royal Society of Chemistry, England , eISBN: 978-1-84755-117-7. 2004.
[19] *Technical Datasheet – Fumatech® FKE*. FuMA-Tech GmbH, Germany.
[20] Chandran, R.R., Chin, T.-T., *Reactor Analysis of a Chlor-alkali Membrane Cell.* Electrochimica Acta, England. 1986.
[21] Larchet, C., Auclair, B., Nikonenko, V., *Approximate Evaluation of Water Transport Number in Ion-Exchange Membranes*. Electrochimica Acta, Elesevier, 2004.
[22] Brown, A.P., Krumpelt, M., Loutfur, R.O., and Yao, N.P., *J.electrochem.Soc. 129, 2481,* 1982.